CTU Journal of Innovation and Sustainable Development
ISSN 2615-9422 | e-ISSN 2815-5602

DOI:10.22144/ctujoisd.2024.269

Calculation of electromagnetic force and temperature distribution of amorphous transformers in different operating modes by finite element method

Pham Hong Hai[1], and Bao Doan Thanh[2*]

[1]School of Electrical and Electronic Engineering, Hanoi University of Science and Technology, Viet Nam

[2]Faculty of Engineering and Technology, Quy Nhon University, Viet Nam

*Corresponding author (doanthanhbao@qnu.edu.vn)

Article info.

Received 27 Jul 2023
Revised 06 Oct 2023
Accepted 17 Oct 2023

Keywords

Amorphous transformer, ansys 3D, finite element method, no load, short circuit, temperature

ABSTRACT

The study used the Finite element method (FEM) by ANSYS 3D software to calculate the distribution of electromagnetic force (EMF) and temperature on the high voltage and low voltage windings (HLVWs) of the amorphous steel core 3 phase transformer (ASCT) which has a power of 1000kVA –22/0.4kV under different load cases: No load, full load and short circuit (SC). The obtained results show the exact temperature distribution and location where the highest temperature is found on the HLVWs of ASCT. From the analysis of the temperature distribution on the HLVWs, it is shown that when the transformer falls into an SC fault, it causes the greatest EMF and thermodynamic force, causing extremely heavy consequences for the transformers. The obtained results help designers, manufacturers, and operators have the most suitable options to improve strength of SC and increase the life of the transformer.

1. INTRODUCTION

In operation, the temperature of the transformer core and windings may rise because of the heating. If the cooling problem is effectively solved, the lifetime of the transformers is increased. The process of heat transfer, conduction, convection, and cooling of oil transformers is very complicated, especially the amorphous steel core transformers (ASCT) (Binh & Doanh, 2011; Hanh et al., 2009; Xiao & Du, 2016). A simulation model for fast and accurate calculation of EMF distribution, and temperature distribution inside and outside the coil or around the oil tank is significant. The accurate determination of the highest temperature points on the coils and oil tanks is essential for ASCT.

ASCT is capable of reducing no-load losses by up to 70% compared to conventional silicon steel core transformers. Therefore, ASCT is widely used and increasingly installed on the power grid. The authors (Roginskaya et al., 2020; Nazmunnahar et al., 2019) confirmed that the ASCT can reduce no load losses and provide higher economic efficiency compared to conventional silicon steel core transformers. Because of the special structure of the steel core and the rectangular of the coil, the electric field distribution, the dissipated magnetic field, the force distribution on the coil, and the heat distribution on ASCT are asymmetric on the same wire ring. The sum of these large thermodynamic stresses is very dangerous for the coil in short-circuit condition (Zhai et al., 2022). Bal et al. (2019), the finite element method (FEM) is used in simulation to analyze the electromagnetic transients of the Ansys three-phase oil type distribution transformer simulation program. Results are presented in terms of losses, voltages, currents and magnetic flux of the transformer. Arjona et al., 2012 calculated the

electromagnetic force (EMF) when a short circuit (SC) occurs using FEM to identify the highest temperature in the core or windings. The analytical or "semi-analytic" methods were used to solve temperature transfer problems and simulate heat distribution in dry transformers using FEM (Hualin et al., 2019). Chen et al., 2019 compared the thermal-circuit model and FEM to verify the validity of the thermal path model for dry-type transformer. Li et al. (2014) performed the 3D temperature distribution simulation of amorphous dry transformer SCBH15-600/10. The method of CFD is applied to simulate the temperature distribution on the windings of a dry-type ASCT 560 kVA-22/ 0.4 kV in different working cases (Bao, 2022). The distributions of the scattered magnetic fields, dissipative reactance and EMF affecting the high voltage and low voltage windings (HLVWs) of the transformer in case of SC are analyzed and calculated using FEM (Bao et al., 2023; Yahiou et al., 2022; Jin et al., 2022).

In the literature, several methods are proposed to calculate and analyze temperature in transformers. The electromagnetic parameters and average temperature parameters are calculated in these thermal research methods. However, the heat distribution in the ASCT may not be investigated. The existing works may not provide an efficient computational process to identify the location of the high temperature on the coils and the combined thermodynamic. Therefore, the primary purpose of this paper is to investigate the electromagnetic process of a 3-phase ASCT with a capacity of 1000kVA – voltage 22/0.4kV using FEM in Ansys Maxwell 3D software. The results of the electromagnetic analysis including magnetic field, current, voltage, and loss as input parameters for thermal analysis can be calculated using CFD software. The temperature distribution around the two windings and the lid of the transformer tank will be analyzed. Then, the position with the highest temperature on the HLVWs of the ASCT in different load cases, such as no-load mode, rated mode, and fault SC mode, will be determined. The obtained results imply that the highest EMF and thermal force will occur in the SC condition of the ASCT. Based on the final results, recommendations for manufacturers and operators are provided to increase the life and high performance of ASCT.

2. SHORT CIRCUIT CURRENT, ELECTROMAGNETIC FORCE AND TEMPERATURE DISTRIBUTION

2.1. Short-circuit current

In case the transformer is working with the nominal primary voltage, if an SC occurs on the secondary side, the SC current will be very large. At this time, the entire nominal voltage is applied to the very small SC impedance of the transformer, so it is called an operating SC. The SC current is as follows:

$$i = I_{SC}\sqrt{2}\left[\sin(\omega t - \psi - \varphi_{SC}) + \sin(\psi + \varphi_{SC}).e^{-\frac{R_{SC}}{X_{SC}}\omega t}\right] \quad (1)$$

where:

- $I_{SC} = \frac{U_{Nominal}}{Z_{SC}}$: SC current (A)
- $\varphi_{SC} = \text{arctg}\frac{X_{SC}}{R_{SC}}$ phase angle (rad)
- U_{Nom}: Nominal voltage (V)
- Z_{SC}: SC impedance (Ω)
- X_{SC}; R_{SC}: SC reactance; resistance (Ω)
- t: time (s)
- ψ: angle at the moment of SC (rad)
- ω: angular frequency (rad/s).

2.2. Electromagnetic force (EMF)

The interaction between current and magnetic flux in the winding region follows the left-hand rule, creating EMF in the transformer winding. According to the Lorentz formula, we write the EMF relationship as (2):

$$F_{dt} = \int_L I.B\sin(\vec{I},\vec{B})dl \quad (2)$$

Or:

$$d\vec{F} = \vec{B}\times\vec{I}dl = \vec{B}\times\vec{J}.ds.dl \quad (3)$$

where:

- I (A): the magnitude of the current; J (A/m^2): the density of the current;
- B (T): the magnetic flux density; F (N): the EMF;
- ds: the area infinitesimal; dl: the length infinitesimal.

2.3. Temperature distribution

2.3.1. The temperature source of the transformer

The main source of heat in the transformer is the magnetic circuit and winding. Core loss and copper loss are the main losses; in addition, there are additional losses such as auxiliary losses on windings and additional core losses that are all turned into heat in the transformer (García et al., 2002; Yüksel, 2016).

– Winding losses:

The winding losses $\Delta P'_u$ caused by alternating current are calculated according to the following formula:

$$\Delta P_u^{'} = mI_1^2R_{1d} + mI_2^2R_{2d} \quad (4)$$

Where m is the number of phases; R_{1d}, R_{2d} are the phase resistances of the HLVWs measured with direct currents, respectively. And I_1, I_2 are the root-mean-square values of the HLVWs transformer currents of the transformer, respectively.

The loss $\Delta P'_u$ in the formula is called the main loss, while the auxiliary loss is usually characterized by the auxiliary loss factor k > 1:

$$\Delta P_u = k_1m_1I_1^2R_{1d} + k_2m_2I_2^2R_{2d} \quad (5)$$

The factor k depends on conductivity and winding construction, frequency, conductor material and temperature.

Core losses include two types: hysteresis losses and Foucault's current losses. The hysteresis loss depends on the chemical composition of the foil, the thickness of the foil, the temperature, the hysteresis period, and the frequency of the magnetizing current.

2.3.2. Heat conductivity

In transformer windings, heat conduction occurs between windings of different temperatures. This heat conduction follows the formula for heat transferred per unit of isothermal surface per unit of time, and it is proportional to the temperature gradient (Arjona et al., 2012; Chen et al., 2019).

$$q = -\lambda\frac{\partial t}{\partial n}\ \left[W/m^2\right] \quad (6)$$

where q is current density (W/m^2)

$\frac{\partial t}{\partial n}$ temperature gradient (K/m)

λ - thermal conductivity (W/m.K)

To establish the differential equation for heat conduction in a medium, we assume that the medium is at rest, isotropic, and physical quantities such as density ρ, specific heat c, and coefficient of thermal conductivity λ are constant.

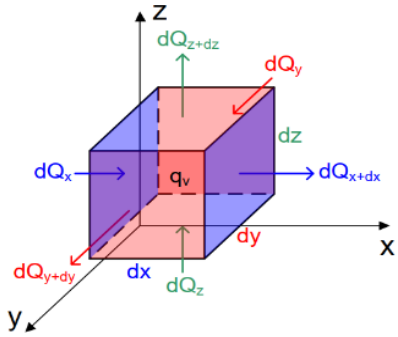

Figure 1. Heat balance for an element with volume dv

The heat flow through the surface (dx, dy) at the z coordinate, in the z direction is determined:

$$dQ_z = -\lambda dxdy\frac{\partial t}{\partial z} \quad (7)$$

The heat flow through the surface (dx, dy) at coordinates z + dz, in the z direction is determined:

$$dQ_{z+dz} = -\lambda dxdy\frac{\partial}{\partial z}\left(t + \frac{\partial t}{\partial z}dz\right) \quad (8)$$

The total amount of heat accumulated in the box in the 3 directions x, y, z is:

$$dQ = \lambda dxdydz\left(\frac{\partial^2 t}{\partial x^2} + \frac{\partial^2 t}{\partial y^2} + \frac{\partial^2 t}{\partial z^2}\right) \quad (9)$$

According to the law of conservation of energy, this heat accumulation is equal to the change in internal energy of the volume element dv per unit time:

$$dQ = C\rho dxdydz\frac{\partial t}{\partial \tau} - dxdydz.q_v \quad (10)$$

Inferred in the case of an internal heat source qv ≠ 0:

$$\frac{\partial t}{\partial \tau} = \frac{\lambda}{C\rho}\left(\frac{\partial^2 t}{\partial x^2} + \frac{\partial^2 t}{\partial y^2} + \frac{\partial^2 t}{\partial z^2}\right) + \frac{q_v}{C\rho} \quad (11)$$

Assume $a = \frac{\lambda}{Cp}(m^2/s)$ is the thermal diffusion conductivity coefficient.

From (11), we have:

$$\frac{\partial t}{\partial \tau} = a\left(\frac{\partial^2 t}{\partial x^2} + \frac{\partial^2 t}{\partial y^2} + \frac{\partial^2 t}{\partial z^2}\right) + \frac{q_v}{C\rho} \quad (12)$$

Solving differential equations of heat conduction (12) needs more conditions on monotherapy; boundary and time. We have the general solution for the heat conduction process.

2.3.3. Convective heat transfer

The convection heat transfer process is described by a system of four differential equations: the convective heat differential equation, the energy differential equation, the motion differential equation, and the continuum equation. This is an analytical method for calculating convective heat dissipation based on solving a system of differential equations describing the process and univalent conditions (Li, Y. et al. 2014; Xiao & Du, 2016).

The differential equation for convective heat transfer:

$$a = -\frac{\lambda}{(t_w - t_f)}\left(\frac{dt}{dn}\right)_{n=0} \quad (13)$$

The energy differential equation represents the relationship between temperature, time, space, and fluid flow rate. Assuming an incompressible, homogeneous fluid, there is no internal heat source and frictional losses are neglected, the equation has the form:

$$\frac{dt}{d\tau} + \omega_x\frac{dt}{dx} + \omega_y\frac{dt}{dy} + \omega_z\frac{dt}{dz} = a\left(\frac{d^2t}{dx^2} + \frac{d^2t}{dy^2} + \frac{d^2t}{dz^2}\right) \quad (14)$$

The differential equation of motion has the form:

$$\rho\frac{d\vec{\omega}}{d\tau} = p\vec{g} - \text{grad}\rho + \nabla^2 \quad (15)$$

The continuity equation (when the fluid is incompressible) has the form:

$$\frac{d\omega_x}{dx} + \frac{d\omega_y}{dy} + \frac{d\omega_z}{dz} = 0 \quad (16)$$

2.3.4. Radiant heat transfer

When the heat source is a magnetic circuit and a transformer winding, there is a heat exchange between them as radiation and converted into heat through the electromagnetic wave medium.

The radiant power of a unit area of the heating surface is calculated according to the Stefan – Boltzmann formula:

$$q_{bx} = k \times v\left(T_{a1}^4 - T_{a2}^4\right) \quad (17)$$

where Ta1 and Ta2 are the absolute temperature of the hot body and the environment, respectively; v - relative radiation coefficient.

The unit of q is (W/m^2), and the units of both T_{a1} and T_{a2} (°K). Constant k = 5.77×10^{-8} (W/m^2.°K^4)

Formula (17) is rewritten:

$$q_{bx} = 5,77v\left[\left(\frac{t_{a1}}{100}\right)^4 - \left(\frac{t_{a1}}{100}\right)^4\right] \quad (18)$$

When the temperature difference $\theta = T_{a1} - T_{a2} = 75°C$, the above formula can be rewritten as:

$$q_{bx} = 2,38v\theta^{1,25}\left(1 + 0,11T_0\right) \quad (19)$$

where T_0 is ambient temperature; θ is the temperature difference between the object to be cooled and the environment; q_{bx} - radiant power per unit area of the heated surface (W/m^2).

2.4. Finite element method using Ansys Maxwell software

Table 1 shows the operation factor of a 1000kVA power transformer from SANAKY at Ha Noi. The detailed dimension is obtained from the drawings provided by the manufacturer.

The operation factor shown in Table 1 and the design dimensions of the transformer are the input data for Ansys 3D. (User's Guide, 2019).

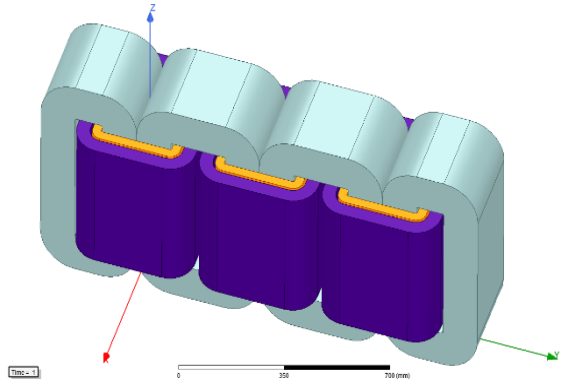

Figure 2. Transformer model used in Ansys Maxwell 3D

Figure 2 shows the transformer model used in Ansys Maxwell 3D.

Ansys Maxwell is copyrighted software package at the computational and simulation room of the Faculty of Engineering and Technology, Quy Nhon University.

Table 1. Operation factor of the ASCT

No.	Factor	Value
1	The number of phases	3
2	Frequency (Hz)	50
3	Capacity (kVA)	1000
4	Winding diagram	Δ/Y
5	Nonimal voltages of high/low winding (kV)	22/0.4
6	Number of turns per phase in high/low (turns)	1400/14
7	Nonimal currents high/low (A)	26.24/1443.4
8	No load current (%)	0.5
9	SC voltage u_k (%)	5.62
10	No load losses ΔP_0(W)	275
11	SC losses ΔP_k (W)	8290

3. RESULTS AND DISCUSSION

3.1. Analysis results in transformer mode with short circuit faults

3.1.1. Short circuit current of HLVWs

With all the dimensions and electrical parameters of the transformer and (1) formula, we can calculate the fault SC current on the windings as follows:

+ SC current on the high voltage winding (high VW) is:

$$i_{SC-HV} = 466.9\sqrt{2}\left[\begin{matrix}\sin(100\pi t - 1.4184) \\ +\sin(1.4184)\times e^{-\frac{-12.04}{80.72}.100t}\end{matrix}\right](A)$$

+ SC current on low voltage winding (low VW) is:

$$i_{SC-LV} = 25683.3\sqrt{2}\left[\begin{matrix}\sin(100\pi t - 1.4184) \\ +\sin(1.4184)\times e^{-\frac{-12.04}{80.72}.100t}\end{matrix}\right](A)$$

Figures 3 and 4 show that the waveform of the short-circuit currents of the HLVWs reaches a maximum (max) value in the first cycle at time t = 34 ms and gradually decreases in the following cycles until reaching steady-state values, with max values shown in Table 2.

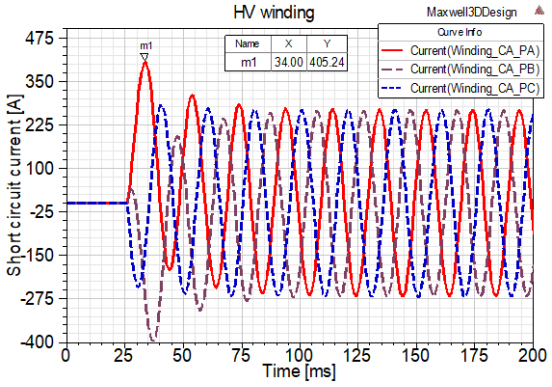

Figure 3. SC current on the high VW

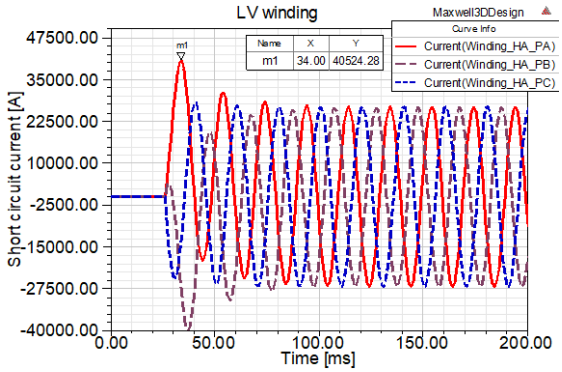

Figure 4. SC current on the low VW

Table 2. Results of max SC current

Parameter	High VW	Low VW
Max SC current I_{maxSC} (A)	405.24	40524.28

At time t = 34 ms, the obtained results show that the max SC current on the max low VW is I_{maxLV} = 40524.28(A) while the amplitude of the rated current is I_{rateLV} = 1443.4(A). This means that the max SC current on the low VW is 28 times higher than the rated current. Similarly, the max SC current on the high VW is I_{maxHV} = 405.24(A) while the amplitude of the level current is I_{rateHV} = 26.24(A). The max SC current on the high VW is 27 times higher than the rated current. The results of the max SC current on the HLVWs of the 1000kVA transformer are used to calculate the SC EMF stress acting on the HLVWs.

3.1.2. Calculate the EMF acting on the HLVWs when the transformer is short circuit

EMF is a quantity representing the internal force generated in the winding under the action of EMF. Stress calculation formula: σ_{stress} = F/A(N/m^2); where F is the force (N) and A is the surface area (m^2). To check the durability of the winding under

dangerous SC conditions, we need to calculate the EMF acting on the winding and then compare it with the allowable stress of the winding.

The results of EMF value on HLVWs are shown in the following figures:

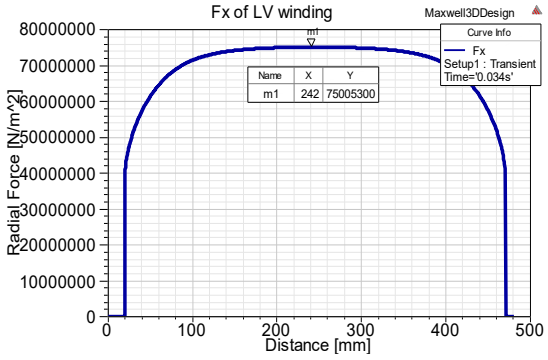

Figure 5. Value of radial force F_x in the low VW

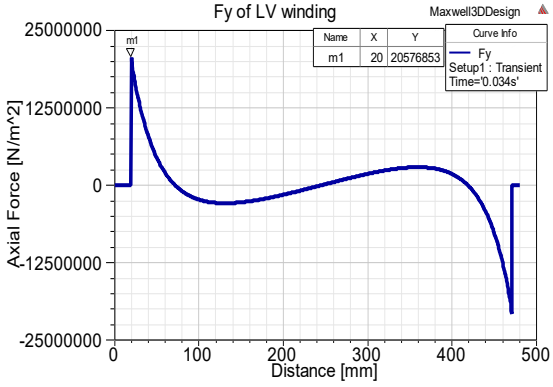

Figure 6. Value of axial force Fy in the low VW

Figures 5 and 6 show the values of the radial EMF F_x and the axial force F_y on the low VW as follows:

+ Max radial force F_x:

$$F_{x\_LV} = 7.5005\times10^7 \text{ N/m}^2$$

+ Max axial force F_y:

$$F_{y\_LV} = 2.0322\times10^7 \text{ N/m}^2$$

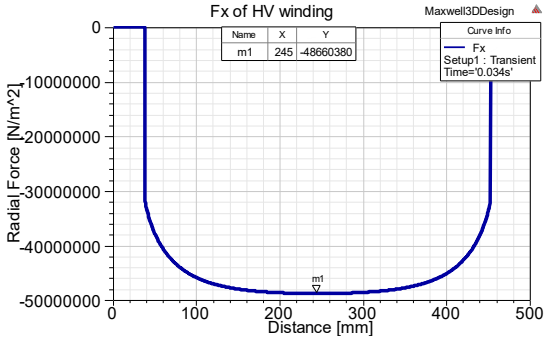

Figure 7. Value of radial force F_x in the high VW

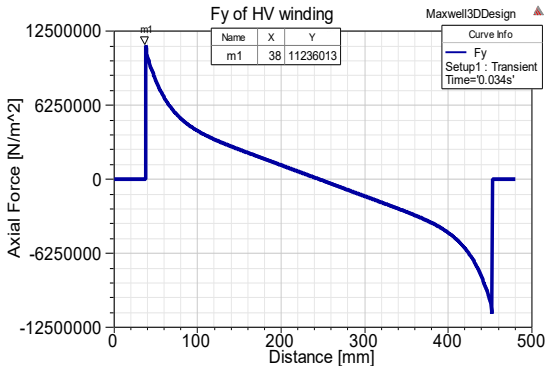

Figure 8. Value of axial force Fy in the high VW

Figures 7 and 8 show the values of the radial EMF F_x and the axial force F_y of the low VW as follows:

+ Max radial force Fx:

$$F_{x\_HV} = 4.8660\times10^7 \text{ N/m}^2$$

+ Max axial force F_y:

$$F_{y\_HV} = 1.1236\times10^7 \text{ N/m}^2$$

In Figure 5, the value of the F_x in the low VW has the smallest value at the two ends of the winding. This force increases in the middle of the winding and gets the max value at the middle of the winding. In Figure 7, the value of F_x in the high VW is similar to the F_x in the low VW, but it is in the opposite direction. The max value is at the middle of the winding. The values of F_y in the HLVWs are shown in Figure 6 and Figure 8. The max values of these forces at the two ends of each winding are defined. These forces become zero in the middle of the windings.

The above results show that the EMF is most concentrated in the outermost edge of the low VW and the innermost edge of the high VW. The value of the total EMF on the HLVWs is shown in Figure 9 and Figure 10.

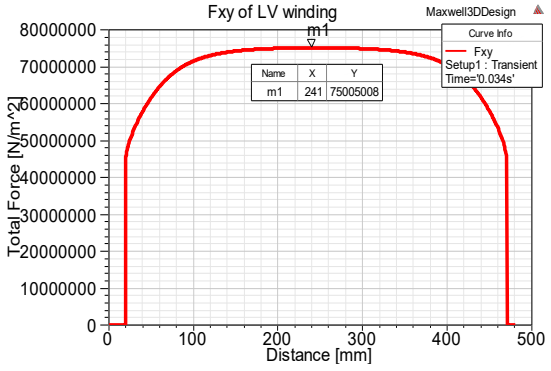

Figure 9. Value of the total max force F_{xy} of the low VW

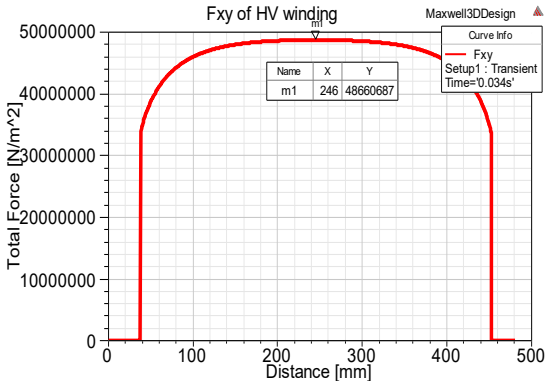

Figure 10. Value of the total max force Fxy of the high VW

In Figure 9 and Figure 10, it can be seen that the position with the largest total EMF value is in the middle of the winding (according to height y) and equal to the value of the max radial EMF.

The value of total EMF on HLVWs is shown in Table 3.

Table 3. Table of max EMF values on HLVWs

Total EMF F_{xymax} (N/m^2)	Low VW	High VW
F_{xmax}	7.5005×10^7	4.8660×10^7
F_{ymax}	2.0576×10^7	1.1236×10^7
F_{xymax}	7.5005×10^7	4.8660×10^7
Allowable stress limit: σ_{ASL}	$(5\div10).10^7$	
Comparing F_{xymax} with σ_{ASL}	$5\times10^7 < 7.5005\times10^7 < 10\times10^7$	

In Table 3, the largest EMF is $F_{xymax} = 7.5005\times10^7$ N/m^2 while the allowable stress of copper wire $\sigma_{ASL} = (5\div10).10^7$N/m^2 (Binh & Doanh, 2011). Therefore, when an SC occurs with the max current on the low VW being $I_{LVmax} = 40524.26$(A), the max EMF of the windings has not exceeded the allowable limit.

When a SC occurs, besides the EMF, the thermodynamic force acting on the transformer windings plays an important role and needs to be considered. The thermodynamic force is closely related to the temperature distribution after the SC moment and is also related to the winding material and the cooling type.

3.2. Result of the calculation of temperature distribution on HLVWs and the tank shell of transformer

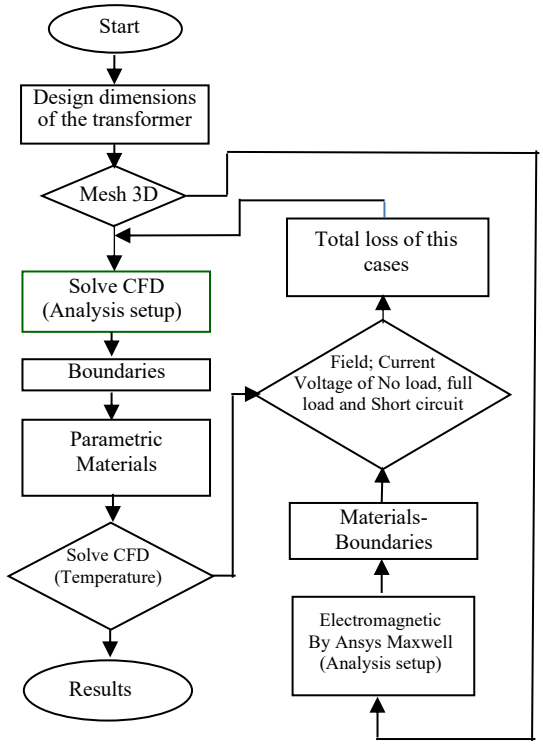

Figure 11. Combination for the CFD - EMF solutions

The FEM, by using the ANSYS software, is used to calculate the distribution of temperature on the windings of a 3-phase ASCT with rated power of 1000kVA.

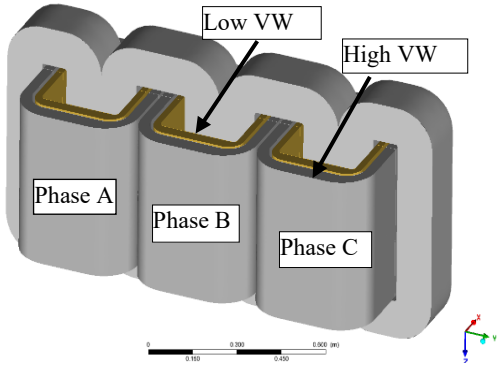

Figure 12. Model of ASCT 1000kVA in CFD software

The total results about loss power of no load, rated load and SC mode, of the EMF simulation are used as input for the thermal simulation CFD. The calculation process by CFD software is depicted in Figure 11 and the model of ASCT 1000kVA in Figure 12.

3.2.1. No load

In the no load, the current of high VW is 0.9A. The loss is 275W at no load. Results of CFD analysis in the temperature distribution on HLVWs as shown in Figure 13.

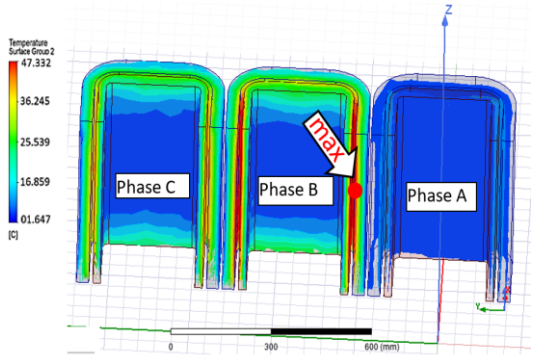

Figure 13. Value of temperature on the HLVWs

Figure 13 shows the results of the analysis of the temperature value on the HLVWs. The point with highest temperature on high VW is 36.2^{0}C and low VW is 47.3^{0}C.

With the results studied above, the heat distribution simulated by CFD software shows that the temperature on the coils has not been uniformly distributed. On the windings the terminal part has a higher concentration distribution of temperature at the bottom. Because, according to heat transfer theory Transformer includes natural convection heat transfer. The temperature flow is upward, creating a warmer temperature layer than below the winding. With the transformer structure, phase B is in the middle of the transformer, so phase B is affected by temperature from next to phase A and phase C. At the same time, the low VW is located inside the high VW, making it more difficult for the air to cool down in the narrow gap between the HLVWs. Finally, the value of temperatures on low VW is higher than that on high VW.

3.2.2. Full load

In Full load, the rated current of low VW is 1443.4(A); high VW is 26.24(A). Results of CFD analysis in the value of temperature on the HLVWs as shown in Figure 14 and Figure 15.

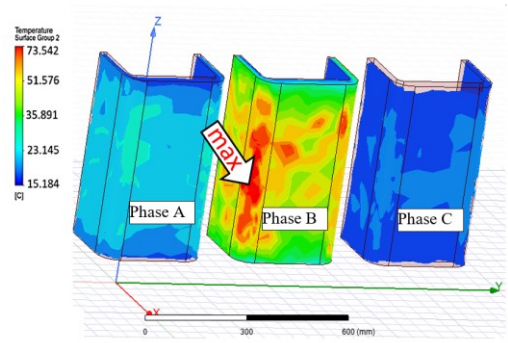

Figure 14. Value of temperature on the low VW

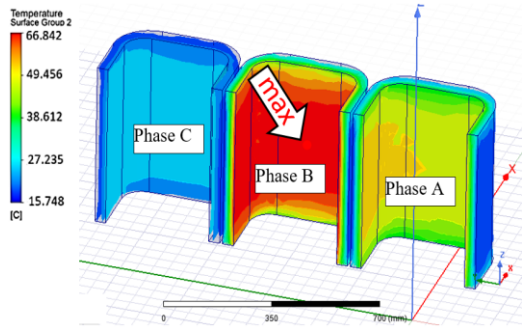

Figure 15. Value of temperature on the high VW

Figure 14 and Figure 15 show the results of the analysis of the temperature values on the two windings. The point with highest temperature on high VW is 66.8^{0}C and that on low VW is 73.5^{0}C.

3.2.3. Short circuit

In SC, obtained simulation results of transformer temperature distribution in case of SC fault in time domain. This simulation is conducted set up for 3s with a time step of 0.01s. The number of meshed elements for this simulation is 15.600.000 elements and requires the problem to converge.

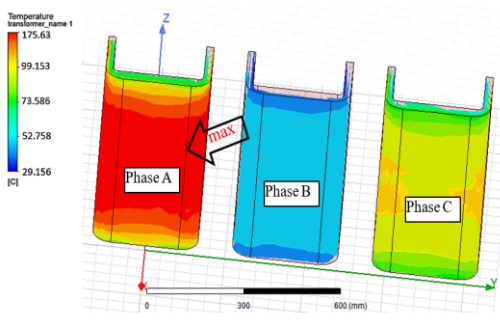

Figure 16. Value of temperature on the low VW

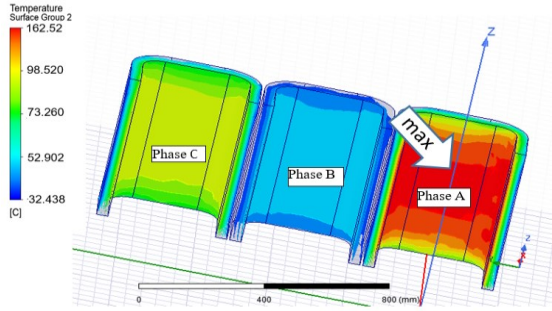

Figure 17. Value of temperature on the high VW

In SC, Figures 16 and 17 show the results of the analysis of the temperature value on the two windings for 3s. These results show that the temperature rise is much higher than the full load. The point with highest temperature on high VW is 162.5^0C and that on low VW is 175.63^0C. This temperature has exceeded the allowable temperature of insulation class F. If maintained for a longer time, it affects the durability and life of the transformer.

We analyzed and compared temperature distributions on the tank surfaces of the transformer in case of no load, full load, and SC. The hottest spots on the tank surfaces are shown in Table 4.

Table 4. Average and max temperature (^{0}C) of transformer in case of no load, full load and SC

Results of Max Temperature (^{0}C)	Test modes		
	No load	Full load	SC
High VW	36.2	66.8	162.5
Low VW	47.3	73.5	175.6

Figure 18 shows the temperature distribution on the oil tank casing of the transformer using the CFD software.

The CFD analysis allows us to determine the different temperature distributions inside and outside the oil tank of the transformer. Figure 18 depicts the temperature value outside the oil tank with the highest temperature of 121.89^0C.

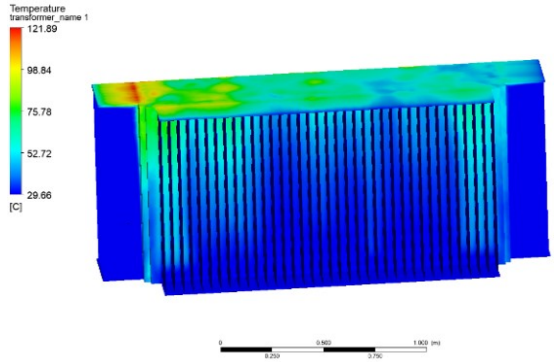

Figure 18. Analysis of temperature distribution on the transformer oil tank

4. CONCLUSION

The research results of this work show that, with ASCT with 3 3-phase SC fault, the EMF acting on the windings has a rather large value. Especially, the thermal stress effects on the windings are considered simultaneously. The windings of the transformer are subjected to a combined force called thermodynamic stress during a SC. This ASCT composite force analysis problem is set in a multi-physical environment that is a combination of mechanical, electrical, and thermal. Solving the problem by analysis method is almost impossible. Therefore, using the FEM through the coupling of Ansys and CFD electromagnetic simulation software is an advantage to help solve the problem quickly and accurately. This helps to determine the position of the max thermal stress on the windings and case accurately, in order to have approaches to strengthen the affected locations so that these transformers are able to tolerate electromagnetic stresses, thermodynamic stress, and total force stress in the case of a SC.

ACKNOWLEDGMENT

This work was supported by the project B2022-DQN-03 sponsored by the Ministry of Education and Training, Viet Nam.

REFERENCES

Arjona, M. A., Ovando-Martínez, R. B. B., & Hernandez, C. (2012). Thermal-fluid transient two-dimensional characteristic-based-split finite-element model of a distribution transformer. *IET Electric Power Applications*, *6*(5), 260-267. https://doi.org/10.1049/iet-epa.2011.0286

Bao, D. T. (2022). Calculation of temperature distribution of air-cooled three-phase dry transformer. *Journal of Science and Technology - University of Danang*, *20*(11.2). 38-43.

Bao, D.T., Tung, D. D., & Ho T. Le. (2023), Computation of Electromagnetic Forces in the Windings of Amorphous Core Transformers,

Archives of Electrical Engineering, *72*(2), 521 –539. https://doi.org/10.24425/aee.2023.145423

Bal, S., Demirdelen, T., & Tümay, M. (2019). Three-Phase Distribution Transformer Modeling and Electromagnetic Transient Analysis Using ANSYS Maxwell. In *2019 3rd International Symposium on Multidisciplinary Studies and Innovative Technologies (ISMSIT)*, (pp. 1-4). IEEE. https://doi.org/10.1109/ISMSIT.2019.8932953.

Binh, P. V., & Doanh, L. V. (2011). *Transformer - theory - operation - maintenance - testing*. Science and Technology Publishing.

Chen, Y., Zhang, C., Li, Y., Zhang, Z., Ying, W., & Yang, Q. (2019). Comparison between thermal-circuit model and finite element model for dry-type transformer. In *2019 22nd International Conference on Electrical Machines and Systems (ICEMS),* (pp. 1-5). IEEE. https://doi.org/10.1109/ICEMS.2019.8922410

García, A., Espinosa-Paredes, G., & Hernández, I. (2002). A thermal study of an encapsulated electrical transformer. *Computers and Electrical Engineering*, *28*(6), 417- 445. https://doi.org/10.1016/S0045-7906(01)00004-0.

Hanh, V.G., Thu, P. T., Ha, T. K., & Sau N. V. (2009). *Electric machine I*. Science and Technology Publishing, Ha Noi.

Hualin, S., Bin, X., Yun, F., & Guohui, L. (2019). Simulation analysis of temperature distribution of oil-immersed self-cooled transformer under different environmental conditions. In *2019 22nd International Conference on Electrical Machines and Systems (ICEMS),* pp. 1-4. IEEE. https://doi.org/10.1109/ICEMS.2019.8922368

Jin, M., Wen, T., Chen, W., Zhao, Y., Wu, J., Wu, X., & Zhang, Q. (2022). Influence of frequency components of short-circuit electromagnetic force on vibration characteristics of power transformer windings. In *2022 IEEE International Conference on High Voltage Engineering and Applications (ICHVE)* (pp. 01-04). IEEE. https://doi.org/doi: 10.1109/ICHVE53725.2022.9961671

Li, Y., Guan, Y. J., Li, Y., & Li, T. Y. (2014). Calculation of thermal performance in amorphous core dry-type transformers. *Advanced Materials Research*, *986*, 1771-1774. https://doi.org/10.4028/www.scientific.net/AMR.986-987.1771.

Nazmunnahar, M., Simizu, S., Ohodnicki, P. R., Bhattacharya, S., & McHenry, M. E. (2019). Finite-element analysis modeling of high-frequency single-phase transformers enabled by metal amorphous nanocomposites and calculation of leakage inductance for different winding topologies. *IEEE Transactions on Magnetics*, *55*(7), 1-11. https://doi.org/10.1109/TMAG.2019.2904007

Roginskaya, L., Yalalova, Z., Gorbunov, A., & Rakhmanova, J. (2020, October). Features of amorphous steel magnetic cores for transformers operating at mains frequency. In *2020 International Conference on Electrotechnical Complexes and Systems (ICOECS)* (pp. 1-5). IEEE. https://doi.org/10.1109/ICOECS50468.2020.9278451

User's Guide. (2019). *ANSYS 3D V16 2019*. REV5.0, p. 1-1011.

Xiao, M., & Du, B. X. (2016). Effects of high thermal conductivity on temperature rise of epoxy cast winding for power transformer. *IEEE Transactions on Dielectrics and Electrical Insulation*, *23*(4), 2413-2420. https://doi.org/10.1109/TDEI.2016.7556520.

Yahiou, A., Mellah, H., & Bayadi, A. (2022). Inrush current reduction by a point-on-wave energization strategy and sequential phase shifting in three-phase transformer. *International Journal of Engineering*, *35*(12), 2321-2328. https://doi.org/10.5829/IJE.2022.35.12C.07.

Yüksel, N. (2016). The review of some commonly used methods and techniques to measure the thermal conductivity of insulation materials. *In Insulation materials in context of sustainability*. IntechOpen. https://doi.org/10.5772/64157.

Zhai, Y., Zhu, R., Li, Q., Wang, X., Gu, Y., & Li, S. (2022, September). Simulation research on electrodynamic force and deformation of transformer windings under short-circuit condition. In *2022 IEEE International Conference on High Voltage Engineering and Applications (ICHVE)* (pp. 1-4). IEEE. https://doi.org/10.1109/ICHVE53725.2022.9961358.